ACS OMEGA

Open Access

http://pubs.acs.org/journal/acsodf

Article

Gas Evolution Principle during Gas Drainage from a Drill Hole along the Coal Seam and Reasonable Borehole Layout Spacing

Yutian Wang,* Xun Zhao,* Pengfei Wang, and Yong Chen

Cite This: *ACS Omega* 2023, 8, 44338−44349

Read Online

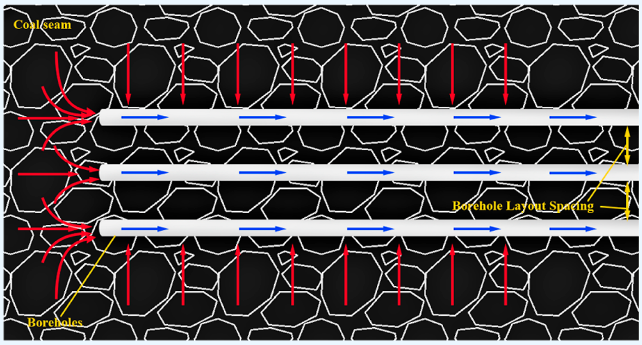

ABSTRACT: The efficiency of coal seam gas drainage can be further improved by the accurate mastery of the gas evolution principle during gas drainage from the drill hole along the coal seam and reasonable optimization of borehole layout spacing. Based on the actual geological conditions of the no. 2 coal seam in a coal mine in Guizhou, China, and relevant control equations, a fluid−structure interaction model of gas drainage from a drill hole along the coal seam was established in this paper. Besides, numerical simulation research on the gas evolution principle during gas drainage along the coal seam and optimization of the borehole layout spacing was carried out with the COMSOL simulation software; and these were verified in combination with the project site. The results showed that in the early stage of gas drainage the gas pressure in the area near the drill holes decreased significantly. As the gas drainage went on, the degree of influence decreased gradually. During the gas drainage from adjacent drill holes, the gas pressure in the coal body between the holes decreased rapidly, and the migration was obvious. With the increase of the spacing between the drill holes, the drainage superposition effect between these holes gradually decreased until the influence area around a single hole is independently distributed in a circle-like shape, indicating that the optimization and the reasonable spacing of the drill holes are directly related to the effect of the gas drainage. With the increase of drilling spacing, the superposition effect of extraction between the holes gradually decreased until the influence area around a single hole is independently distributed in the shape of a circle, indicating that the optimization of drilling spacing is directly related to the effect of gas drainage. The results of numerical simulation were verified by analyzing the three-dimensional map of the gas pressure during the period of gas drainage at the project site and by comparing and examining the rational borehole layout spacing of the drill hole along the coal seam. The results of this study can be used to determine the spacing of gas extraction boreholes and improve the efficiency of gas extraction in the no. 2 coal seam of a coal mine in Guizhou, China, as well as to provide a reference for the gas pressure evolution, velocity field distribution, the prediction of effective drainage area, and the selection of rational borehole layout spacing during gas drainage.

1. INTRODUCTION

Most of the coal mines in China adopt underground mining, while gas disasters seriously restrict the safe production of mines.[1−5] Gas exists as an underground disaster, but it is a clean energy itself. If utilized efficiently, it can reduce the occurrence of underground gas disaster accidents and provide clean energy for human society.[6−10] Therefore, in the process of coal resources mining, gas drainage is often used as the main technical means to reduce the pressure and content of coal seam gas underground and to ensure the safe and efficient production of coal mines.[11−13]

At present, a number of scholars have emerged to enrich underground gas drainage technology by adopting various research means. Yu and Gao[14] analyzed the application of the gas drainage technology of large diameter boreholes in highly gassy mines. This technology can control well the gas concentration in the upper corner of the working face and the gas concentration in the return air. Ma et al.[15] solved the problem of gas prevention and control in the fully mechanized caving face of the hard top slab of extra thick coal seam in the Jiaoping mining area by the roof directional long borehole segmental hydraulic fracturing technology. Yan and Yan[16] effectively solved the problem of low permeability of no. 2 coal seam in the Shuanglong coal mine by ultrasonic penetration enhancement technology. Guo[17] performed fracturing and permeability enhancement on the coal seam by deep hole

Received: September 27, 2023
Revised: October 26, 2023
Accepted: October 27, 2023
Published: November 9, 2023

https://doi.org/10.1021/acsomega.3c07456
ACS Omega 2023, 8, 44338−44349

presplitting blasting technology, which effectively improved the gas drainage efficiency of Houcun coal mine. In numerical simulations, Liu et al.[18] combined the theory of mining-induced fissure "O" ring and "ring-shaped fissure body" and used numerical simulations to reveal the mechanism of increasing gas outflow from a fully mechanized coal face caused by double unloading in the process of comprehensive working face mining. Cheng et al.[19,20] concluded that the effect of negative pressure on increasing the concentration of gas drainage decreases with time by solving the flow-solid coupling model of gas drainage. Zhang et al.[21] drew the conclusion that the gas concentration increases with the increase of seal length and drill hole diameter from the numerical simulation calculation by a two-media coupling model. Wang et al.[22] established a multimechanism fluid−structure interaction model of coal seam gas with the COMSOL software to better reveal the nature and law of gas migration in loose and low permeability coal seams during gas drainage. Saki et al.[23,24] gave the design parameters such as a drill hole diameter and drainage pressure of the gas drainage pipeline by CFD numerical simulations to improve the safety production efficiency of the mine.

According to previous studies, the effectiveness of gas drainage depends on various aspects, including the method used in gas drainage and the physical properties of the coal body itself (porosity and fracture rate, permeability, degree of metamorphism, etc.),[25−27] and the design parameters of drainage. Gas drainage parameters include borehole length, borehole diameter, borehole spacing, the drainage time, and the negative drainage pressure.[28−31] Borehole layout parameters are important parameters that affect the gas drainage compliance as well as the gas drainage efficiency.[32−34] In terms of gas drainage drilling arrangement, Liu et al.[35] used the area method to optimize the uncovering borehole layout in the coal seam to successfully solve the problems of large amount of drilling work, long drainage period, and poor drainage effect during rock cross-cut coal uncovering in the coal seam. Jiang et al.[36] performed numerical simulations with the fluid−structure interaction model and comprehensively analyzed the change rule of effective drainage radius of drill hole along the coal seam without the influence of faults in combination with the on-site borehole gas drainage amount method. Fan[37−39] optimized the borehole layout parameters of high level gas drainage by means of on-site mining parameters and effectively solved the problem of gas overlimit in the upper corner. Chen et al.[40,41] established a coal seam gas drainage model with the COMSOL software to optimize the borehole layout spacing in coal seam gas drainage drill holes, which provided some theoretical guidance for on-site construction. Fan et al.[42] used COMSOL and FLAC software to solve the numerical model interactively to optimize the spacing of the boreholes in the protected coal seam. Whittles et al.[43] obtained the optimal spacing of gas drainage drill holes with a numerical simulation model in a longwall coal mining face in a mine in the UK. Gurbanov et al.[44] demonstrated that the correct choice of borehole spacing can effectively exclude the void zone during drainage.

Previous researchers have carried out a great number of studies on the effective drainage radius and the layout of drainage drill holes, but most of them are based on two-dimensional planar models; there is a lack of three-dimensional (3D) models; and only a small amount of literature has investigated the specific quantitative methods for optimizing the spacing of the drill holes by means of numerical simulation. In this study, the COMSOL numerical simulation software was used to study the gas drainage from the drill hole along the coal seam, analyze the evolution principle of gas pressure, the distribution of gas migration velocity field, and the volume change of the effective exploration area, and combine with the on-site measurement to give a more accurate borehole layout spacing. This study provides some theoretical guidance for the rational design of drill holes along the coal seam in the no. 2 coal seam of a mine in Guizhou, China.

2. MODELING

2.1. Mathematical Model.

2.1.1. Basic Assumptions. Based on the characteristics of coal seam gas occurrence, the following assumptions are made:[45−47]

(1) The coal seam is a dry porous medium.
(2) The coal seam is a uniform and isotropic medium, and the influence of the anisotropy of the coal seam on permeability orientation is neglected.
(3) The temperature change in the gas flow field is small, and the transport of gas in the coal seam is treated as an isothermal process.
(4) The fractures in the coal seam are filled with free gas, while the gas in the matrix exists in both adsorbed and free states.
(5) The gas is considered an ideal gas, and its dynamic viscosity remains unchanged under isothermal conditions.
(6) Both the pore system and the fracture system are continuous medium systems.

2.1.2. Mass Equation of Gas Occurrence. When the mass of gas occurrence is calculated, the coal body system is generally divided into two parts: the pore system and the fracture system. The gas mass in the two systems is summed to obtain the total mass of gas occurrence in the unit volume of coal can be expressed as eq 1[48]

$$m = \frac{V_L p_m}{p_m + P_L} \rho_a \frac{M_c}{V_M} + \varphi_m \frac{M_c}{RT} p_m + \varphi_f \frac{M_c}{RT} p_f \tag{1}$$

where m is the total gas content per unit volume of coal, kg; V_L is the Langmuir volume, the maximum adsorption capacity of the monomolecular layer, m^3; P_L is the Langmuir pressure, the adsorption equilibrium pressure when the adsorption capacity is half of the maximum adsorption capacity, MPa; ρ_a is the apparent density of coal, kg/m^3; p_m is the gas pressure in the pore system, MPa; T is the Kelvin temperature of the coal seam, K; M_c is the molar mass of methane molecular, kg/mol; V_M is the molar volume of methane in the standard state, m^3/mol; p_f is the gas pressure in the fracture system, MPa; φ_m is the porosity,%; φ_f is the fracture rate,%; and R is the ideal gas constant, J/(mol·K).

2.1.3. Gas Diffusion Governing Equation of Coal Matrix. Gas diffusion in coal seams is mainly driven by vapor phase diffusion, and the driving force for diffusion is the concentration difference of vapor phase gas between pores and fractures in the coal matrix,[49] During the process of gas extraction, the adsorbed gas in the coal matrix acts as a mass source and desorbs outward, making diffusion and permeation continue to operate. The formula for the mass exchange flux between the coal matrix and the fracture system can be expressed as eq 2

https://doi.org/10.1021/acsomega.3c07456
ACS Omega 2023, 8, 44338−44349

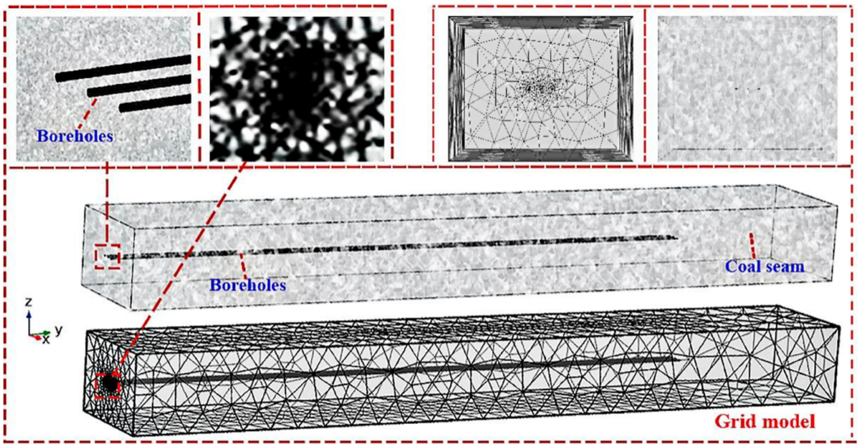

Figure 1. 3D model of coal seam gas predrainage.

$$Q_s = D\sigma_c(c_m - c_f) \quad (2)$$

where Q_s is the mass exchange rate of gas between the pore system and the fracture system in the unit volume of coal, kg/(m^3·s); D is the gas diffusion coefficient, m^2/s; σ_c is the matrix shape factor, m^{-2}; c_m is the concentration of vapor phase gas in the pores, kg/m^3; and c_f is the concentration of vapor phase gas in the fractures, kg/m^3.

According to the characteristics of gas migration, the mass exchange rate of gas between the pore system and the fracture system is actually the change of the mass of the pore system with time, that can be expressed as eq 3

$$\frac{\partial m_1}{\partial t} = -\frac{\sigma_c D M_c}{RT}(p_m - p_f) \quad (3)$$

where m_1 is the mass of gas in the pore system, kg; t is time, s.

The governing equation of the pore system, i.e., the governing equation of the gas pressure in the matrix changing with time, can be obtained, as shown in eq 4

$$\frac{\partial p_m}{\partial t} = -\frac{\sigma_c D V_M(p_m - p_f)(p_m + P_L)^2}{V_L RTP_L\rho_a + \varphi_m V_M(p_m + P_L)^2} \quad (4)$$

2.1.4. Governing Equation of Gas Seepage in Fractures. The gas seepage in the fracture system conforms to the mass conservation equation. It can be expressed as eqs 5 and 6[50]

$$\frac{\partial(\varphi_f\rho_f)}{\partial t} = -\nabla(\rho_f v^*) + Q_s(1 - \varphi_f) \quad (5)$$

$$\rho_f = \frac{M_c}{RT}p_f \quad (6)$$

where v^* is the gas seepage velocity in the fracture, m/s.

The gas in the fracture flows in the Darcy seepage mode, and the gas seepage velocity conforms to the following equation

$$v^* = -\frac{k_e}{\mu}\nabla p_f \quad (7)$$

where k_e is the effective porosity of the coal seam, m^2; and μ is the gas dynamic viscosity coefficient, Pa·s.

2.1.5. Porosity Change Equation. The porosity change equation can be expressed, as eqs 8 and 9[51]

$$\frac{\varphi}{\varphi_0} = 1 + \frac{1}{M\varphi_0}(p - p_0) + \frac{V_L}{3\varphi_0}\left(\frac{K}{M} - 1\right)\left(\frac{p}{P_L + p} - \frac{p_0}{P_L + p}\right) \quad (8)$$

$$M = E(1 - v)/(1+v)(1 - 2v) \quad (9)$$

where p is the gas pressure in the coal seam; p_0 is the initial gas pressure in the coal seam, Pa; φ is the porosity of the coal seam; φ_0 is the initial porosity of the coal seam,%; E is the elastic modulus, MPa; $K = E/3(1 - 2v)$ is the bulk modulus; and v is the Poisson's ratio.

2.1.6. Stress Field Control Equation. Assuming that the adsorbed gas diffusion in the coal body conforms to Fick's law, the gas seepage in the coal seam conforms to Darcy's law and the deformation of the coal body is tiny. Based on the equilibrium property of force and the adsorption desorption property, the equation of the stress field can be expressed as[51−54]

$$Gu_{i,ij} + \frac{G}{1 - 2v}u_{j,ji} - \left[\alpha + \frac{KV_LP_L}{(P_L + p)^2}\right]p_{,i} + f_i = 0 \quad (10)$$

where $G = E/2(1 + v)$ is the shear modulus; $\alpha = 1 - K/K_s$ is the Biot coefficient; K_s is the skeleton elastic modulus; u is the displacement; $u_{i,ij}$ is the tensor form; and the first subscript i indicates the i-direction component of u; the second subscript i indicates the i-direction partial derivative of u_i; and the third subscript j indicates the j-direction partial derivative of $u_{i,i}$, $p_{,i}$ is the sign of the derivation expressed in the tensor form in the mechanics; and f is the volume force.

2.2. Geometric Model and Boundary Conditions. The no. 2 coal seam of a mine in Guizhou, China, was selected as the study object to establish a 3D model of gas drainage from a drill hole along the coal seam, with a height of 10 m, a width of 15 m, and a depth of 100 m. Three parallel cylinders were excised in the center of the model to represent the drill holes with a diameter of 96 mm and a depth of 80 m. The spacing between the three drill holes is 1 m (Figure 1). In this model, the free tetrahedral structure was selected to dissect the grid. The total number of grid cells are 101,773. The maximum grid cell size is 3.5 m; the minimum cell size is 0.15 m; and the curvature factor is 0.3.

The stress in the vertical direction of the geometric model is 10 MPa. The displacement of the bottom surface and the left and right sides is 0; and the front and back surfaces are set as free displacement. The mass source is distributed in the whole geometric model; the initial pressure is the initial gas pressure of the actual coal seam, and some physical parameters of the model are shown in Table 1.

Table 1. Partial Physical Parameters of the Model

parameter	numerical value
initial porosity φ_0	0.037
initial permeability k_0/m^2	1.00×10^{-17}
Klinkenberg factor/Pa	1.44×10^5
initial gas pressure of coal seam p_0/Pa	1.00×10^6
Langmuir constant (pressure) P_L/Pa	3.03×10^6
Langmuir constant (volume) V_L/m^3	20
Poisson's ratio ν	0.3
modulus of elasticity E/MPa	2800
coal matrix modulus of elasticity E_s/MPa	8400
coal matrix density ρ_s/kg·m^{-3}	1350

3. NUMERICAL SIMULATION RESULTS AND ANALYSIS

In order to analyze the specific rules of the fluid−structure interaction model of gas drainage from a drill hole along the coal seam, this study was mainly carried out in four aspects: gas pressure evolution, displacement field distribution, velocity field distribution, and volume of effective drainage area.

3.1. Gas Pressure Evolution. The changes in the gas pressure evolution of different durations during gas drainage from drilling along the coal seam are shown in Figure 2, with the 3D effect on the left side and the *YZ* plan view on the right side. As seen from the left side of Figure 2, from the beginning of drainage to 180 days, the color changed significantly, indicating that there was a significant reduction in gas pressure; especially in the area near the drill holes, the color appeared light blue, which indicates that the pressure of the coal body around the drill holes had been released. The feasibility of the method of gas drainage from drill hole along coal seam was verified. Meanwhile, according to the right side of Figure 2, the red is deeper from the bottom of the drill hole to the bottom of the coal body, indicating that arranging the holes along the coal seam only from one side had a minor impact on the reduction of gas pressure in the coal body behind the drill hole. Therefore, the holes should be arranged alternately from both sides to increase the gas drainage efficiency.

Combined with the results in Figure 2 at different times, the color of the area near the drill hole became lighter gradually with the increase of time after the beginning of gas drainage from the drill hole along the coal seam, indicating that with the gas drainage from drill holes, the gas pressure in the nearby coal seams may be reduced. From the 3D effect on the left side of Figure 2, the influence area of the drill hole is distributed in a quasi-circular shape near the drill hole. At 30 d, the superimposed effect of extraction between adjacent drill holes is not obvious; and the *YZ* view on the right side shows that the top and bottom sides of the drill holes are reddish-brown in color; and the yellow and blue areas are very light; as time goes on, the impact area of extraction in each drill hole is gradually enlarged, and there is a certain tendency of compounding the impact area at 90 d. The color of the red areas on both sides of the top and bottom sides of the drill holes appears lighter in the *YZ* view, while the blue and especially the yellow areas are enlarged. The influence area of each drill hole and the composite area is further enlarged at 180 d. The change tendency indicates that with the increasing of the extraction, the drainage effected area is gradually enlarged and the drainage superimposed effect is increasingly obvious.

To further illustrate the time-dependent properties of gas pressure evolution, the gas pressure data at nodes (7, 2, and 5) are summarized at different times, and the results are shown in Figure 3. The curves in Figure 3 show a gradually decreasing trend and become smoother and smoother with the increase of the drainage time, indicating that at the early stage of gas drainage, due to the pressure difference between the coal seam gas pressure and the drilling holes as well as the role of the negative pressure of the drill holes, the coal seam gas pressure decreased rapidly, but with the passage of the drainage time, the coal seam gas pressure decreases continuously. In the later stages of extraction, the difference between the matrix gas pressure and the fracture gas pressure tends to a fixed value, which leads to a gradual stabilization of the gas pressure decrease. This study has some limitations and does not consider the attenuation characteristics of the negative pressure at the mouth of the hole to the bottom of the hole when gas is

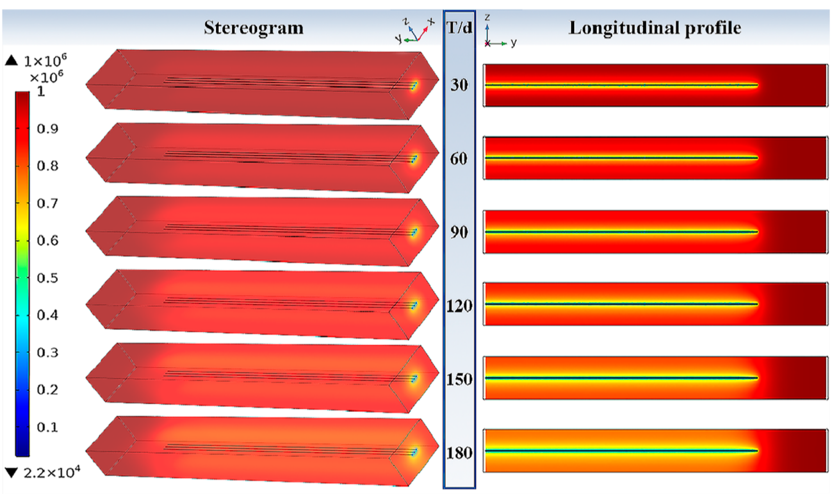

Figure 2. Changes in the gas pressure.

https://doi.org/10.1021/acsomega.3c07456
ACS Omega 2023, 8, 44338−44349

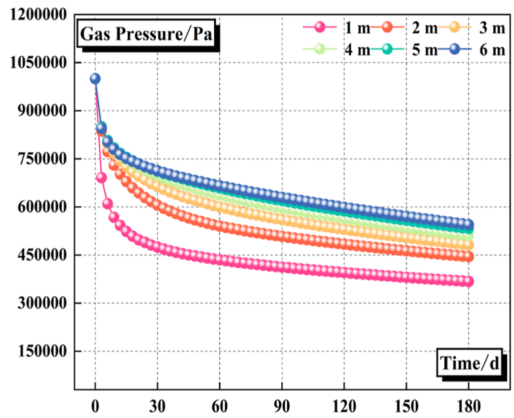

Figure 3. Variation of gas pressure at node (7, 2, 5).

extracted from the borehole.[55] The actual gas extraction results in pressure loss during the flow of gas fluid in the borehole due to a long-track frictional resistance loss, accelerated pressure drop, mixing loss due to the inflow of gas from the borehole wall, and localized resistance loss.[56,57]

3.2. Displacement Field Distribution.

The results of the displacement field distribution of the fluid−structure interaction model of the drill hole along the coal seam are shown in Figure 4. First, from the overall distribution of the displacement field, due to the addition of the initial load above the coal body, the whole shows a downward trend and the coal body structure is compressed. It is found from the *YZ* view (Figure 4b) and combining it with the magnitude of change in the displacement in the *Z* direction (Figure 4c) that the overall displacement in the *Z*-direction does not change greatly. *Z*-direction displacement decreases rapidly in the first 30 days (Figure 4c), begins to rise slowly, and tends to be stable after 45 days, indicating that in the early stage of extraction. Due to gas pressure relief, the increase in effective stress leads to compression of the coal skeleton, which is directly manifested as a decrease in displacement in the *Z*-direction. When the coal seam gas pressure drops to the critical desorption pressure, the adsorbed gas in the coal seam starts to desorb into the pore and fissure channels, resulting in the coal matrix starting to shrink, which leads to a slight lift in the *Z*-direction displacement. As the drainage time reaches 150−180 d, the gas seepage enters a stable phase, and the displacement gradually tends to stabilize.

3.3. Velocity Field Distribution.

Figure 5 shows the gas migration velocity distribution during gas drainage from a drill hole along the coal seam. It can be seen that there is a more obvious blank area from the bottom of the drill hole to the bottom of the coal body when at 30 and 60 days (Figure 5b), indicating that the influence of the drill hole on the bottom of the coal body is small at the early stage of gas drainage. As the gas drainage goes on, the gas in the coal body is gradually drained. The gas from the bottom of the drill hole to the bottom of the coal body begins to migrate; and the Dasi velocity flow line basically covers the whole coal body.

From the 3D distribution of the velocity field (Figure 5a) and the *YZ* plan view, it can be obviously seen that the velocity flow line is obviously "*x*" when the distances between the drill holes are 1 and 2 m; when the distances between the drill holes are 3 m and especially 4 m, the velocity flow line changes, indicating that the drill holes begin to produce the effect of the local unit. The change is more obvious when the distances between the drill holes are 5 and 6 m. This change tendency indicates that the coupling effect between the drill holes is more pronounced when the drill hole spacing is small. As the drill hole spacing increases, each drill hole shows a separate zone of influence. This suggests that there is an effective radius of extraction for the drill holes, and the extraction efficiency of the drill holes on the coal body gas will be greatly reduced when the spacing is greater. In terms of the magnitude and order of magnitude of the change (Figure 5c), when the gas drainage time is within a small scale, the velocity change has little effect on the extraction of the coal body gas. However, if

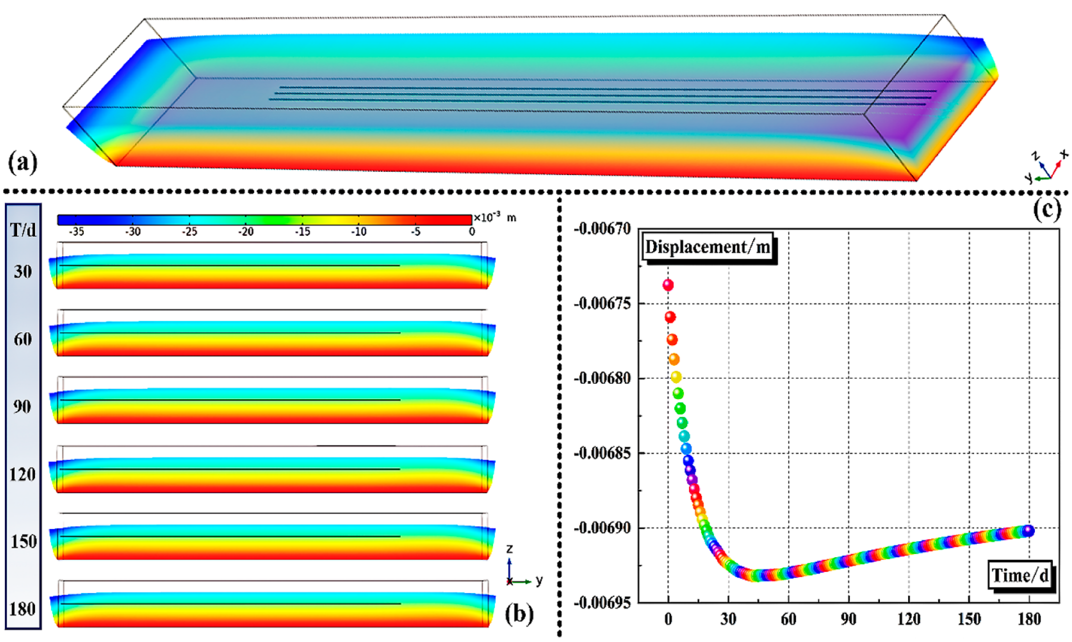

Figure 4. *Z*-direction displacement field distribution results; (a) overall distribution; (b) *YZ* view of displacement field distribution at different times; and (c) displacement change graph at the (2, 2, 2) node.

https://doi.org/10.1021/acsomega.3c07456
ACS Omega 2023, 8, 44338−44349

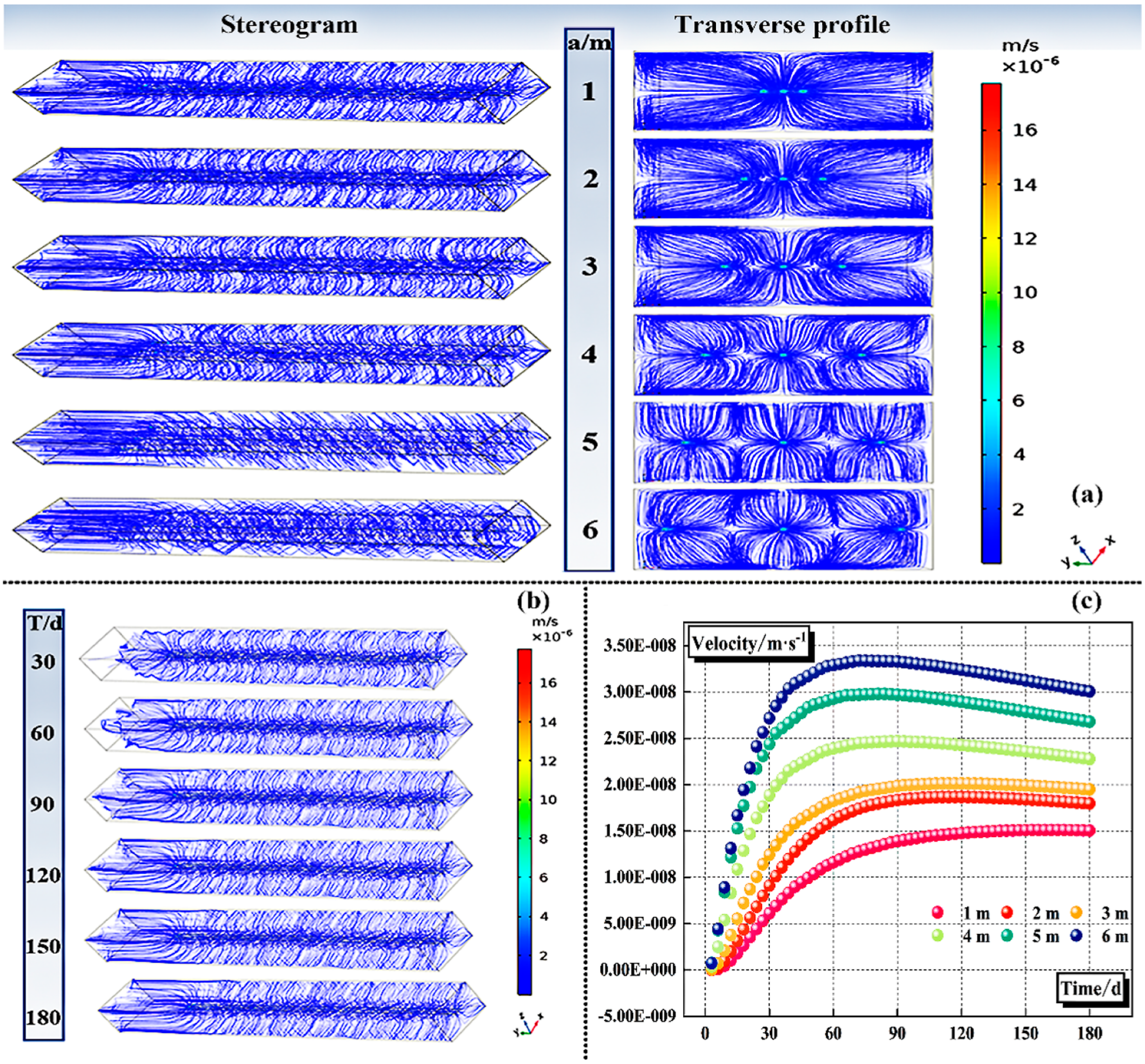

Figure 5. Gas migration velocity field distribution results; (a) velocity field distribution with different borehole layout spacings; (b) velocity field distribution over time with 1 m borehole layout spacing; and (c) velocity volume change at the node.

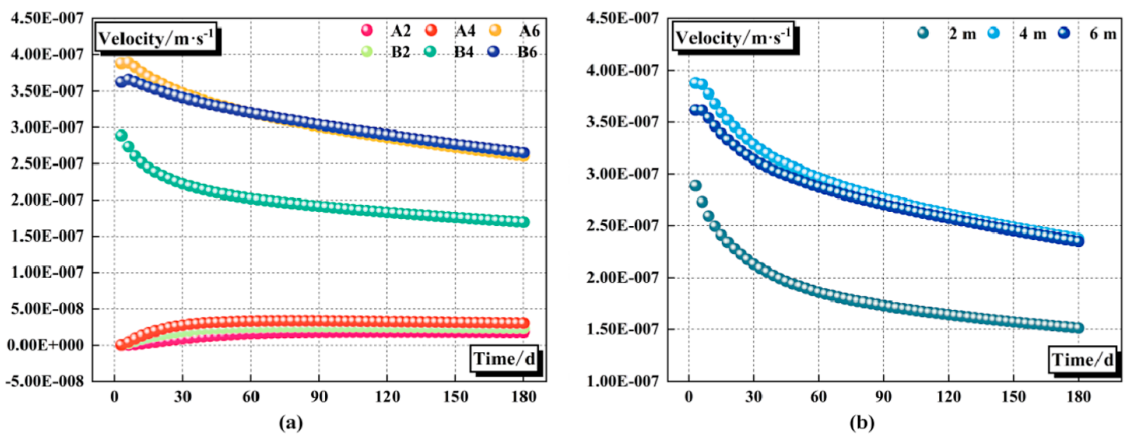

Figure 6. Velocity control results at different nodes; (a) velocity variation at different nodes and (b) comparison of velocity difference at different nodes.

zoomed out to a whole day or a few days, the effect of this velocity change on the extraction of coal body gas is more obvious. In the first 60 d, the gas migration velocity increases rapidly due to gas pressure relief and stabilizes with the increase of gas drainage time and the stabilization of the coal body structure. This aging characteristics lead to the fact that the gas drainage time cannot be neglected in the study of gas drainage. The comparison of the gas migration velocity under

https://doi.org/10.1021/acsomega.3c07456
ACS Omega 2023, 8, 44338−44349

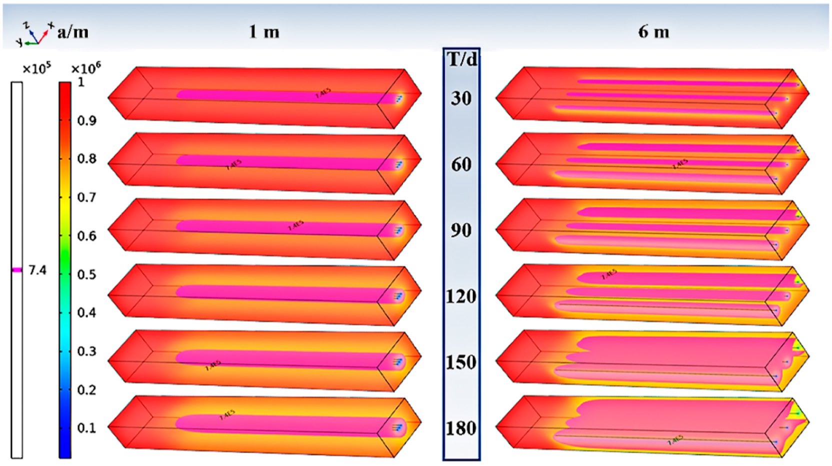

Figure 7. Comparison of effective drainage area between 1 and 6 m drill hole spacing at different times.

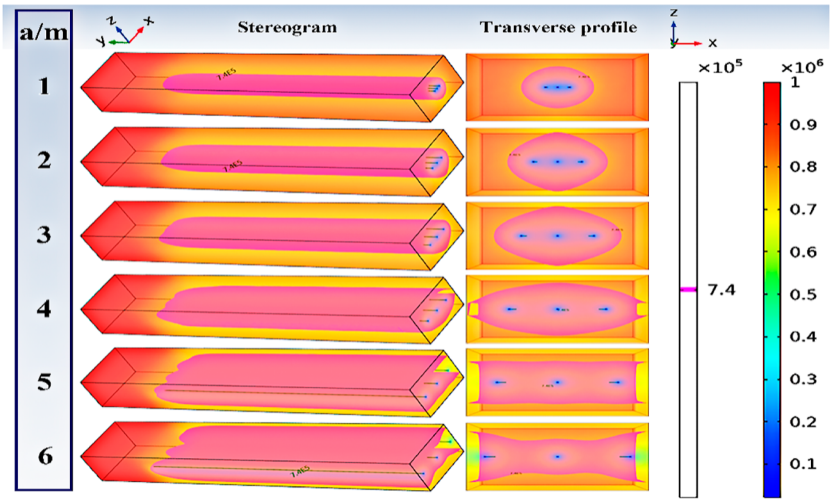

Figure 8. Gas pressure evolution and effective drainage area distribution under different drill hole spacings.

different drill hole spacings shows that the gas migration velocity increases with the increase in the drill hole spacing. The reason is that the node position (2, 2, 2) is in the lower left corner of the *YZ* plane; as the drill hole spacing increases, the left drill hole gets closer to the node; and its gas migration velocity increases accordingly.

In order to compare the gas migration velocity between drill holes and the gas migration velocity farther away from the drill holes more intuitively, the node (2, 2, 2) is denoted as A and the node (7, 2, 5) is taken as B. Nodes A and B are taken at 2, 4, and 6 m borehole layout spacing, respectively. The results are summarized in Figure 6a. The differences between different nodes at the corresponding borehole layout spacing are summarized in Figure 6b. Figure 6 shows the comparison of the velocity variation and difference values at different nodes. The velocity in group B is significantly higher than that in group A (Figure 6a), which indicates that the coupling effect between the drill holes indeed leads to a higher gas migration velocity, thus enhancing the extraction efficiency. The velocity in group B is lower when the drill hole spacing is 2 m than that when it is 4 and 6 m. This is because group B is located between two holes; the holes on both sides have an effect on this location, and this effect is reduced when the drill holes are farther apart. Adjacent borehole extraction, the coupling relationship of adjacent borehole extraction occurs under a certain time and space relationship; the migration rates of coal body methane gas are related to coal body property parameters; it is mainly manifested by the inherent properties, such as the degree of coal body metamorphism, gas content, and permeability characteristics, as well as the combined influence of factors, such as effective stress and matrix shrinkage effect of the coal body as the gas drainage time progresses. The three curves (Figure 6b) all show a decreasing trend, which represents that the difference of the gas migration velocity between the two nodes gradually decreases with the increase of the gas drainage time, which can also partly confirm that in the late stage of gas drainage, with the gas pressure relief of the coal seam, the fissure structure of the coal body pore becomes more and more stable.

3.4. Optimization of Drill Hole Spacing. The spacing of the drill holes is an important factor affecting the efficiency of gas drainage. Too large of a spacing will result in more blind zones, making it impossible to completely reduce the gas pressure in the extraction area to the safety limit. Too small of a spacing between drill holes will result in a waste of manpower and financial resources, thus increasing the cost of gas drainage. Therefore, optimizing the spacing of drill holes is particularly important in gas drainage. Usually, the effective drainage radius of the drill holes is used as a reference for determining the spacing of the drill holes. According to the regulations, the area

https://doi.org/10.1021/acsomega.3c07456
ACS Omega 2023, 8, 44338−44349

where the gas pressure is reduced to less than 0.74 MPa is regarded as the effective extraction area of the drill holes.

It shows the comparison of the effective drainage area at different times when the spacings of the drill holes are 1 and 6 m (Figure 7). From the order of the time increment, the longer the time, the larger the effective drainage area of the drill hole, regardless of the spacing of the drill holes. Comparing the two sets of pictures, when the borehole layout spacing is 1 m, i.e., when the borehole layout spacing is small, an equivalent surface of 0.74 MPa wraps around three drill holes, which indicates that the coupling between the drill holes is stronger with a smaller borehole layout spacing. When the drill hole spacing is 6 m, i.e., when the drill hole spacing is larger, the effective pumping area in the first 120 days is distributed in a circle-like shape around the respective drill holes, and only when the pumping time is too long does it gradually expand so as to be linked together, which indicates that the coupling effect between drill holes decreases significantly when the drill hole spacing is too large.

Figure 8 shows the front view of the gas pressure and effective extraction area with different drilling spacings at 180 days of gas drainage. The gas pressure near the drill holes is small when the drill hole spacing is 1 m, while the gas pressure is larger at the left and right ends away from the drill holes (Figure 8). At the same time, the blue color near the drilling line, especially in the position between the drill holes, shows that the gas pressure decreases faster between the drill holes, which is due to both of the surrounding drill holes having an effect on that position. As the spacing between the drill holes increases, the superimposed drainage effect between the drill holes diminishes and will eventually be distributed in a quasi-circular pattern around the respective drill holes. The yellow color shown at the left and right edges in the last three figures is not the color of the isotimic surface but the color of the coal body surface. Comprehensively, the six figures show that the area below 0.74 MPa is larger when the spacing of the drill holes is about 4−5 m. When the spacing of drill holes is 6 m (Figure 8), it can be seen that the upper and lower ends are not covered by the drainage area, and there is a large drainage blind area.

In order to better determine the change in the effective area volume, the effective area volume in Figure 8 is integrated, and the curve results are shown (Figure 9). The effective area volume will gradually increase as the drainage time goes on and after reaching the peak value, it slowly decreases and tends to stabilize (Figure 9). It indicates that the effective area volume will tend to a stable value with the gradual stabilization of the coal body structure and thus converge during the drilling gas drainage. When the drainage time is about 40 days, the effective area volume is the largest when the borehole spacing is 3 m, indicating that the drainage effect is better when the borehole spacing is 3 m at the early stages of drainage (Figure 9). When the drainage time is 180 days and the drill spacing is 4 m, the effective area is the largest (Figure 9). At the same time, the highest peak value of the effective area volume curve under different drill hole spacings is 5 m; however, the highest peak value of the effective area volume is basically similar between 4 and 5 m drill hole spacings, and after 120 d of the drainage time, the effective area volume curve of the effective area curve with 5 m drill hole spacing decays more obviously. Comparing the earliest peak time of the effective area volume under the three kinds of drilling spacings of 4, 5, and 6 m, and synthesizing the results of the analysis in Figure 8, the results further show that the gas drainage effect of the mine's no. 2 seam is optimal when the drilling spacing is 4−5 m.

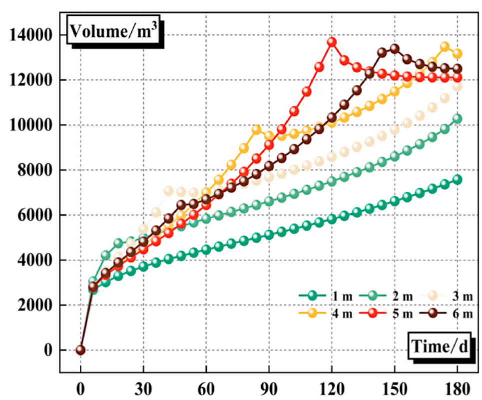

Figure 9. Effective area volume change curve.

4. FIELD APPLICATION

In order to verify the numerical simulation results and to ensure the reliability of the test results, field inspections were carried out on the no. 2 coal seam with the spacings of 3, 4, and 5 m between drill holes. The borehole layout is a drill hole along the coal seam and the drilling spacing *r* is arranged according to 3, 4, and 5 m, respectively. Each group is arranged with 6 drill holes; and each group is spaced 40 m apart. The borehole diameter is 96 mm; and the drilling length is 80 m. The drilling inclination is arranged according to the inclination of the coal seam; and the arrangement of the test drill holes is shown in Figure 10.

The construction of the test drill holes in the same study section is completed within 2 days, and the sealing work is completed within 24 h. The test drill holes are sealed by the same two plugging and one injection sealing process as the daily drainage in the mine. After sealing the test holes, the network was completed within 24 h. The drainage holes in the same section were connected to the same manifold, with the water discharge device and orifice plate flowmeter device connected at the outlet of the manifold and connected to the drainage pipeline. Based on the observation and statistics of the drainage parameters of each group of test drill holes during the 30 d inspection period, the average extraction amount of each drill hole was calculated and the characteristic curves were plotted, as shown in Figure 11a−c. According to the attenuation characteristics of gas drainage in each group of test holes, the attenuation coefficients and initial drainage quantities at different hole spacings were fitted, as shown in Figure 11d.

Through the characterization of the attenuation coefficients and initial drainage quantities for different borehole layout spacings, the attenuation degree of gas drainage gradually decreases with the increase of arrangement spacing, which are 0.050, 0.032, and 0.027, respectively; the attenuation degree of the borehole layout spacing of 3 m is obviously greater than that of the borehole layout spacings of 4 and 5 m, which means that the coupling effect of the neighboring drill holes during the drainage period is obvious under the smaller spacing of the drill holes; the trend of attenuation degree changes obviously with the increase of the borehole layout spacing. The trend of the attenuation degree decreases with increasing spacing, indicating that the increase in spacing leads to a reduction in

https://doi.org/10.1021/acsomega.3c07456
ACS Omega 2023, 8, 44338−44349

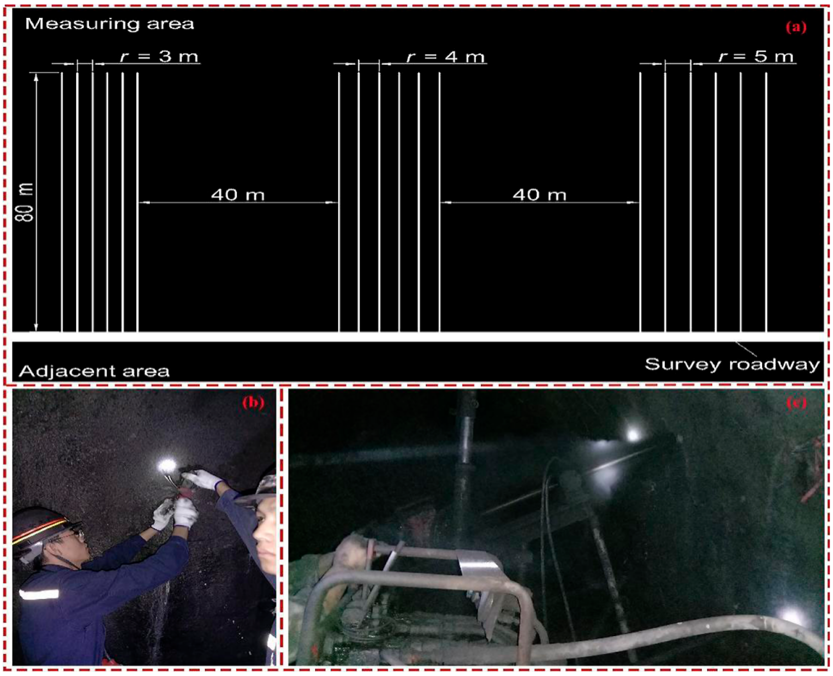

Figure 10. Field test; (a) test program; and (b,c) testing site.

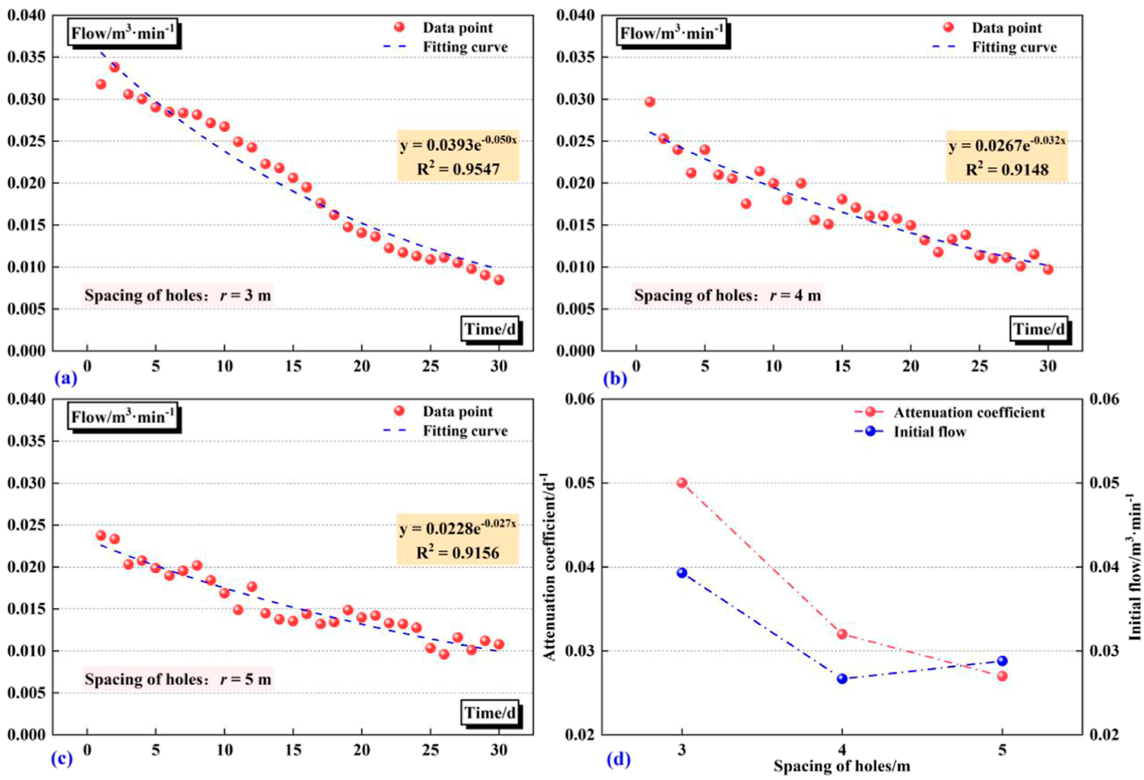

Figure 11. Characteristic curves of average drainage amount, drainage attenuation coefficient, and initial drainage amount under different spacings of hole arrangement; (a−c) characteristic curves of average drainage amount of a single hole; and (d) characteristic curves of drainage attenuation coefficient and initial drainage amount.

the range of the same time limit of the drill holes, and it is necessary to prolong the pumping to achieve the effect of coupling. With the increase of borehole layout spacing, the initial flow of gas drainage from drill holes decreases to 0.0393, 0.0267, and 0.0288, respectively; the attenuation degree of borehole layout spacing of 3 m is significantly larger than that of hole arrangement spacing of 4 and 5 m, which indicates that under smaller borehole layout spacing, the coupling effect of the adjacent drill holes during the drainage period contributes to the reduction of the gas content of the coal seam, and the gas content of coal beds is extracted faster under the same aging characteristics. The initial flow of gas drainage increases

https://doi.org/10.1021/acsomega.3c07456
ACS Omega 2023, 8, 44338−44349

from 0.0267 to 0.0288 when the borehole layout spacing increases from 4 to 5 m, and the difference between the coal seam and the gas deposit in the site may lead to a certain increase or decrease, but the variation interval is very small, which indicates that the further increase of the borehole layout spacing has a limited effect on the initial gas drainage effect.

By fitting the obtained drainage attenuation coefficient and initial drainage amount, the integration results of drainage amount of each group of test holes with different aging characteristics in 30, 60, 90, 120, 150, 180, 210, 240, 270, and 300 days by mathematical integration method are shown in Table 2, and the extraction pattern of different aging characteristics is shown in Figure 12.

Table 2. Integration Results of Extraction Volume under Different Aging Characteristics

time/d	spacing of holes/m		
	3	4	5
30	0.611	0.515	0.469
60	0.747	0.712	0.677
90	0.777	0.788	0.77
120	0.784	0.816	0.811
150	0.786	0.828	0.830
180	0.786	0.832	0.838
210	0.786	0.833	0.842
240	0.786	0.834	0.843
270	0.786	0.834	0.844
300	0.786	0.834	0.844

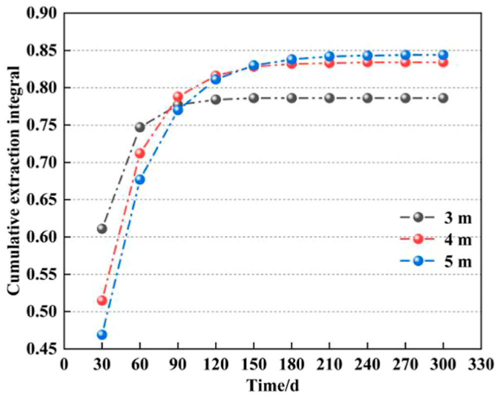

Figure 12. Extraction law of different aging characteristics.

According to the integral results of the drainage volume under different aging characteristics, the drainage equilibrium is reached in 150 d when the spacing of the hole arrangement is 3 m; the drainage equilibrium is reached in 240 d when the spacing of the hole arrangement is 4 m, but basically tends to be stabilized in 180 d; the drainage equilibrium is reached in 270 d when the spacing of the hole arrangement is 5 m, but basically tends to be stabilized in 210 d; from the comparison, it can be found that the drainage equilibrium time of the spacing of the hole arrangement is shorter than that of the spacings of the hole arrangement of 4 and 5 m, and the drainage volume equilibrium is smaller than the cloth hole spacing of 4 and 5 m, which may bring higher gas drainage benefits in a shorter period of time but cannot play a better role in the continuous action mechanism of drilling for coal seam gas drainage. In the spacing of 4 to 5 m, the drainage equilibrium time basically is in the range of 150–210 d, of which 180 d basically reach the drainage equilibrium inflection point.

Through the comprehensive analysis of the drainage attenuation coefficient and the initial drainage characteristics of different hole spacings, as well as the integral results of the extraction under different time characteristics, and combined with the longer time characteristics of drilling gas drainage, the reasonable hole spacing is 4–5 m, which is not only able to effectively extract the coal seam gas but also able to promote the drilling project to play to a reasonable level, which is effectively verified by the numerical simulation results through the field test.

5. CONCLUSIONS

In this study, by combining the actual situation of the no. 2 coal seam in a mine in Guizhou, China, numerical simulation and on-site application were used to optimize the spacing of drill holes in the mine, and it was concluded that the best effect is achieved when the reasonable spacing of drill holes was 4–5 m. In addition, the following conclusions are drawn from this study: (1) gas drainage does affect the structural stability of the coal body, and the *Z*-direction displacement field decreases and slightly increases with the passage of time and finally tends to be stabilized. (2) When extracting from multiple drill holes, the coupling effect of the drill holes will lead to a significantly higher gas migration rate between the drill holes than outside the drill holes, thus improving the gas drainage efficiency; the smaller the distance between the drill holes, the stronger the drainage effect of the drill holes on both sides, and the enhancement of the effect in the opposite direction will lead to a reduction of the gas migration rate between the drill holes, which will lead to the lowering of the gas drainage efficiency to some extent. (3) The volume of the effective extraction area will increase with the increase of gas drainage time, the effective extraction area is distributed in a quasi-circular shape around the drill hole when a single drill hole is extracted, and the size of the spacing between the drill holes will affect the coupling effect between the drilling holes, thereby affecting the spatial morphology of the effective extraction area.

■ ASSOCIATED CONTENT

Data Availability Statement

The data underlying this study are not publicly available due to privacy of contract. The data are available from the corresponding author upon reasonable request.

■ AUTHOR INFORMATION

Corresponding Authors

Yutian Wang – *School of Resources Environment and Safety Engineering, Hunan University of Science and Technology, Xiangtan 411100, China;* orcid.org/0009-0008-2407-7244; Email: wang845858103@163.com

Xun Zhao – *Guizhou Mine Safety Scientific Research Institute Co., Ltd., Guiyang 550025, China; Guizhou Coal Mine Design Research Institute Co., Ltd., Guiyang 550025, China;* Email: limberck@yeah.net

Authors

Pengfei Wang – *School of Resources Environment and Safety Engineering, Hunan University of Science and Technology, Xiangtan 411100, China; Safety Production Laboratory for Gas and Roof Disaster Control of Nanfang Coal Mine,*

https://doi.org/10.1021/acsomega.3c07456
ACS Omega 2023, 8, 44338−44349

Hunan University of Science and Technology, Xiangtan 411100, China

Yong Chen − *School of Resources Environment and Safety Engineering, Hunan University of Science and Technology, Xiangtan 411100, China; State Key Laboratory of Gas Disaster Monitoring and Emergency Technology, Chongqing 400037, China;* orcid.org/0000-0003-1134-4223

Complete contact information is available at: https://pubs.acs.org/10.1021/acsomega.3c07456

Author Contributions

Conceptualization, Y.W.; methodology, Y.W.; software, Y.W.; validation, Y.W., Y.C. and X.Z.; formal analysis, Y.C.; investigation, X.Z.; resources, P.W.; data curation, Y.W.; writing—original draft preparation, Y.W.; writing—review and editing, X.Z.; visualization, P.W.; supervision, P.W.; project administration, X.Z.; and funding acquisition, X.Z.

Funding

This research was funded by A Science and Technology Plan Supported by Guizhou ([2021] General 349), A Science and Technology Plan Supported by Guizhou ([2023] General 360). This research was supported by the Guizhou Province Coal Mine Safety and Efficient Mining Technology Support and Service Talent Base Fund.

Notes

The authors declare no competing financial interest.

■ ACKNOWLEDGMENTS

This research was funded by A Science and Technology Plan Supported by Guizhou ([2021] General 349), A Science and Technology Plan Supported by Guizhou ([2023] General 360). This research was supported by the Guizhou Province Coal Mine Safety and Efficient Mining Technology Support and Service Talent Base Fund.

■ REFERENCES

(1) Sun, Q. G. Research on status quo and prevention countermeasures of coal mine gas disaster in China. *J. China Coal* **2014**, *40* (3), 116−119.

(2) Li, R. Z. Gas governance technology of high-gas driving face in Maojiazhuang coal mine. *Coal Eng.* **2022**, *54* (1), 80−83.

(3) Zhang, C. L.; Wang, E. Y.; Xu, J.; Peng, S. J. A new method for coal and gas outburst prediction and prevention based on the fragmentation of ejected coal. *Fuel* **2021**, *287*, 119493.

(4) Guo, J. Review and prospect of mining technology and equipment of underground coal mines in China. *China Coal* **2021**, *47* (2), 24−30.

(5) Zuo, S. J.; Wang, C. W.; Liao, Y.; Peng, S. Q.; Ma, Z. Q.; Zhang, L. Mechanism of a novel ultrasonic promoting fracturing technology in stimulating permeability and gas extraction. *Energy Rep.* **2022**, *8*, 12776−12786.

(6) Guofu, L. I.; Choa, L. I.; Chunxiu, H.; Zhiming, Y.; Diankun, Z.; Chaoshuai, W.; Zheng, W. Key technology and engineering demonstration for cascade utilization of gas in key coal mining areas of Shanxi Province. *Coal Geol. Explor.* **2022**, *50* (9), 6.

(7) Li, L. Research on Ventilation Safety Management and Gas control Technology in coal mine. *Min. Equip.* **2022**, *4*, 217−219.

(8) Kang, Y. S.; Geng, Z.; Liu, B.; Chen, J. Study on gas extraction efficiency using in-seam borehole method considering influence of plastic zone induced by borehole drilling. *Geomech. Energy Environ.* **2023**, *33*, 100426.

(9) Chen, T.; Meng, Q. R.; Gao, L.; et al. Numerical simulation on coal seam gas extraction based on microwave heat injection. *Min. Res. Dev.* **2022**, *42* (6), 98−104.

(10) Yan, F. Z.; Wang, Y. H.; Zhou, J.; et al. Effect of electric pulse on functional groups and methane adsorption characteristics of anthracite coal. *Saf. Coal Mine* **2022**, *53* (4), 7−12.

(11) Chunli, Y.; Xiangchun, L.; Yanbin, R.; Yiliang, Z.; Feifei, Z. Statistical analysis and countermeasures of gas explosion accident in coal mines. *Procedia Eng.* **2014**, *84*, 166−171.

(12) Shi, J. T.; Wang, S.; Wang, K.; Liu, C.; Wu, S.; Sepehrnoori, K. An accurate method for permeability evaluation of undersaturated coalbed methane reservoirs using early dewatering data. *Int. J. Coal Geol.* **2019**, *202*, 147−160.

(13) Li, Z.; Wang, E.; Zheng, A.; et al. Research on testing technology of deformation and failure of boreholes in coal seam gas drainage and its application. *Coal Sci. Technol.* **2020**, *48* (10), 37−44.

(14) Yu, Y.; Gao, J. Application of large diameter borehole gas drainage technology in high gas mine. *Shandong Coal Sci. Technol.* **2022**, *40* (1), 118−121.

(15) Ma, Y.; Wu, J.; Feng, R.; et al. Pressure relief gas drainage by directional drilling hydraulic fracturing in hard roof. *Min. Saf. Environ. Prot.* **2022**, *49*, 52−56.

(16) Yan, G. F.; Yan, Z. G. Practice on ultrasonic antireflection coal seam and gas extraction in Shuanglong Coal Mine. *Shaanxi Coal* **2022**, *41* (6), 178−182.

(17) Guo, Y. D. Application of deep-hole pre-splitting blasting in gas drainage at working face. *Jiangxi Coal Sci. Technol.* **2022**, *04*, 183.

(18) Liu, C.; Sun, B. Q.; Li, S. G.; et al. Distribution characteristics of fractured rock in overburden induced by double pressure relief mining of thick coal seam and pressure relief gas extraction technology. *Saf. Coal Mine* **2021**, *52* (12), 89−96.

(19) Cheng, Y.; Dong, J.; Li, W.; Chen, M. Y.; Liu, K.; Zhao, W. Effect of negative pressure on coalbed methane extraction and application in the utilization of methane resource. *J. China Coal Soc.* **2017**, *42* (6), 1466−1474.

(20) Guo, X.; Xue, S. Optimization study on negative pressure of gas extraction in directional drilling of ultra thick coal seam. *Min. Res. Dev.* **2021**, *41* (2), 144−148.

(21) Zhang, J.; Liu, Y. W.; Ren, P. L.; Han, H.; Zhang, S. A fully multifield coupling model of gas extraction and air leakage for in-seam borehole. *Energy Rep.* **2021**, *7*, 1293−1305.

(22) Wang, D.; Tang, J.; Wei, J.; et al. A fluid-solid coupling model of coal seam gas considering gas multi-mechanism flow and a numerical simulation analysis of gas drainage. *J. China Coal Soc.* **2023**, *48*, 1−13.

(23) Saki, S. A.; Brune, J. F.; Khan, M. U. Optimization of gob ventilation boreholes design in longwall mining. *Int. J. Min. Sci. Technol.* **2020**, *30* (6), 811−817.

(24) Gilmore, R. C.; Marts, J. A.; Brune, J. F.; Saki, J. S.; Bogin, G. E.; Grubb, J. W. Simplifying CFD modeling of longwall gobs with a modular meshing approach. *Min. Eng.* **2015**, *67* (3), 68−72.

(25) Zhang, B. C. Evolution of crack field in No.3 coal roof of Chengzhuang coal mine and its effect on high-efficiency drainage of gas. M.Sc. Thesis, China Coal Research Institute, 2018.

(26) Zhao, X. J. Study on technology of gas extraction on goaf based on fracture zone distribution law. *Shandong Coal Sci. Technol.* **2018**, *02*, 88−90.

(27) Sheng, L.; Haohao, Z.; Chaojun, F.; Huijie, B.; Zhenhua, Y.; Mei, T. A flow-solid coupling model considering matrix methane seepage for coal methane extraction. *China Saf. Sci. J.* **2018**, *28* (3), 114−119.

(28) Lv, D. N.; Zhang, M. B.; et al. Parameters optimization and engineering application of gas drainage drilling. *Coal Chem. Ind.* **2017**, *40* (10), 127−129.

(29) Zhao, Z. M.; Dong, W.; Wei, G. Y.; Shi, T. W. Numerical simulation study and application of hectometre borehole gas flowrate. *J. Min. Saf. Eng.* **2018**, *35* (2), 436−441.

(30) Hu, L. P. Study on main controlling factors and influencing laws of gas extraction effect in long borehole of roof. M.Sc. Thesis, China Coal Research Institute, 2017.

(31) Shang, H. Application and principle of ZKC5 gas extraction parameter measuring instrument. *Sci. Technol. Inf.* **2017**, *15* (16), 108−109.
(32) Yang, F.; Li, P.; Su, W.; Zhang, J.; Wang, L.; Guo, T.; Wang, S. Study on reasonable gas extraction radius based on multi-index and multi-method. *Energy Rep.* **2022**, *8*, 287−294.
(33) Zhang, B.; Xie, X. G.; Xu, S. Q. Numerical simulation on gas drainage and borehole arrangement parameters of bedding borehole in a coal mine. *J. Mine Autom.* **2018**, *44* (11), 49−56.
(34) Zhao, X. S.; Liu, Y. B.; Shen, K.; et al. Influence factors analysis of coal seam drainage effect and its technical countermeasures. *Saf. Coal Mine* **2019**, *50* (1), 179−183.
(35) Liu, J.; Wu, Z.; Zhang, L.; Wei, Y. Optimization of coal uncovering boreholes layout in gently inclined coal seam based on area method. *J. Saf. Sci. Technol.* **2022**, *18* (04), 113−119.
(36) Jiang, M.; Kang, X. T.; Yan, C. X.; et al. Study on effective extraction radius of bedding borehole under the impact of normal fault. *J. Mine Autom.* **2022**, *48* (02), 55−60.
(37) Fan, F. J. Study on optimal layout of high level gas drainage drilling in goaf of high gas working face. M.Sc. Thesis, China University of Mining and Technology, Xuzhou city Jiangsu province, 2021.
(38) Li, H. Q.; Shi, J.; Hou, J. L. Optimization of layout parameters of high level gas drainage boreholes in fully mechanized top coal caving face. *Shandong Coal Sci. Technol.* **2021**, *39* (7), 119.
(39) Cao, X. Q.; Li, K.; Yao, M. Z. Layout optimization of large diameter high fracture boreholes in separated roadway of fully mechanized top coal caving face. *Coal Mine Mod.* **2021**, *30* (6), 75.
(40) Chen, D.; Lu, P.; Yu, T. Simulation and optimization of effective drainage radius for group hole gas drainage borehole. *J. Hubei Polytech. Univ.* **2022**, *38* (02), 27−31.
(41) Li, Y. T.; Ma, J. K.; Zhao, Z. L. Research on reasonable spacing of directional long distance drilling based on COMSOL simulation. *Coal Technol.* **2020**, *39* (10), 107−112.
(42) Fan, Z.; Fan, G. W.; Zhang, D. S. Representation of mining permeability and borehole layout optimization for efficient methane drainage. *Energy Rep.* **2021**, *7*, 3911−3921.
(43) Whittles, D. N.; Lowndes, I. S.; Kingman, S. W.; Yates, C.; Jobling, S. The stability of methane capture boreholes around a long wall coal panel. *Int. J. Coal Geol.* **2007**, *71* (2−3), 313−328.
(44) Gurbanov, R. S.; Musayeva, S. A.; Gurbanov, R. S.; Ahmedov, Z. Advanced Well Spacing System Application in the Development of Oil and Gas Fields. *Proc. Comput. Sci.* **2016**, *102*, 446−452.
(45) Qin, Y.; Liu, P.; Hao, Y. Mathematical model and dimensionless numerical simulation of methane flow in a dual-porosity and dual-permeability coal seam. *Chin. J. Rock Mech. Eng.* **2017**, *36* (1), 43−52.
(46) Wang, Y.; Yang, L.; Fan, C. Effective drainage area and parameter optimization of bedding drilling in high gas and thick coal seam. *Saf. Coal Mine* **2022**, *53* (10), 212−221.
(47) Zhu, Y. C. Research on anti-outburst technology of drilling pre-pumping gas zone along strata in Tucheng coal mine. M.Sc. Thesis, Guizhou University, Guiyang city Guizhou province, 2021.
(48) Wang, L. Study on numerical simulation of effective radius and borehole extraction scheme of bedding drainage. M.Sc. Thesis, Kunming University of Science and Technology, Kunming city Yunnan province, 2021.
(49) Liu, Q. Q. Damage and permeability evolution mechanism of dual-porosity coal under multiple stress paths and its application. Ph.D. Thesis, China University of Mining and Technology, Xuzhou city Jiangsu province, 2015.
(50) Xu, G.; Zhang, K.; Fan, Y. Numerical simulation of effective drainage radius and optimization of hole spacing under the influence of stack effect. *Min. Saf. Environ. Prot.* **2021**, *48*, 91−96.
(51) Chen, Y.; Chu, T. X.; Chen, P.; Tang, Y. Quantitative study of 3D numerical simulation on optimizing borehole layout spacing of gas drainage. *Coal Geol. Explor.* **2021**, *49* (3), 11.
(52) Fan, Y. F. Research on determination method of effective radius of gas extractin in bedding borehole and optimization of parameters of hole arrangement. M.Sc. Thesis, Xi'an University of Science and Technology, Xi'an city Shaanxi Province, 2019.
(53) Xue, W. C. Study on gas drainage technology of No.9 coal seam in Wuhushan mine. M.Sc. Thesis, China University of Mining and Technology, Xuzhou city Jiangsu province, 2020.
(54) Zhang, C. Study on effects of coal-permeability anisotropy on gas drainage performance: a case study in Baode coal mine. M.Sc. Thesis, Anhui University of Science and Technology, Huainan city Anhui province, 2020.
(55) Zhang, X. B.; Wang, H.; Yang, M.; et al. Study and application on influence mechanism of instability and collapse of drainage borehole on gas drainage. *J. China Coal Soc.* **2023**, *48* (8), 3102−3115.
(56) Wang, Z.-M.; Xiao, J.-N.; Wang, X.-Q.; Wei, J.-G. Experimental study for pressure drops of variable mass flow in horizontal wells. *J. Exp. Fluid Mech.* **2011**, *25* (5), 26−29.
(57) Wang, K. Research on negative pressure distribution law and its application of drilling for consequent landslide gas extraction. M.Sc. Thesis, China Coal Research Institute, 2014.

https://doi.org/10.1021/acsomega.3c07456
ACS Omega 2023, 8, 44338−44349